GFD 2006 Project
Glancing Interactions of Internal Solitary Waves

Dan Goldberg
Advisor: Karl Helfrich

March 15, 2007

Abstract

The Extended Kadomtsev-Petviashvili (eKP) equation is studied as a model for weakly two-dimensional interactions of two-layer solitary waves. It is known that closed forms for two-soliton solutions to the Kadomtsev-Petviashvili (KP) equation can be found by means of Hirota's bilinear transform, but it is determined that no such solution can be found for eKP. A numerical model is developed that agrees with analytical results for reflection of KP solitary waves from a wall. Numerical reflection experiments are carried out to determine whether nonlinear eKP interactions lead to amplitude increases similar to those seen in KP interactions. It is found that when the cubic nonlinear term is negative, the interaction amplitude does not exceed the maximum allowed amplitude for an eKP solitary wave solution, except in the case where the incident wave amplitude is close to this maximum amplitude. When coefficient of the cubic nonlinear term is positive, stationary solutions that are qualitatively different than those of the KP equation are found.

1 Introduction

Long water waves whose amplitudes are small compared to the mean depth are quite common in many geophysical settings, such as free surface disturbances and as interfacial disturbances in a 2-layer system (internal waves). Solitary waves have an extensive history of observations in such settings. Attempts at describing such waves have led to many simplified models. Among the simplest is the Korteweg de Vries (**KdV**) equation for unidirectional propagation. The KdV equation captures the important aspects of long, finite-amplitude waves: nonlinear steepening due to advection and dispersion from nonhydrostatic pressure.

Additional effects can be included by small modifications to the KdV equation. If transverse variation is small but nonzero, the Kadomtsev-Petviashvili (**KP**) equation can be used. One can view the KP equation as a model for three dimensional interactions of long waves. (The term 'three dimensional' is misleading although it is standard – though the KP equation is derived by considering depth variation, it describes a function independent of the vertical coordinate.) On the other hand, if unidirectional internal waves are being considered and the mean layer depths are nearly equal, the Extended KdV (**eKdV**) equation, which

includes cubic nonlinearity, is a better asymptotic approximation to the governing equations. It is also a useful phenomenological model for large-amplitude waves. Combining the two effects results in the Extended KP (**eKP**) equation. The inclusion of both effects in a model is advantageous because internal solitary waves occur with some regularity where currents flow over bathymetry, as do three dimensional interactions of these waves. The modeling of such interactions using the eKP equation is the focus of this study.

In the following two sections, the above equations are given and known closed-form solutions are discussed, as are limitations of the machinery used to generate those solutions. Then in subsequent sections, a numerical model to study three dimensional interactions of internal waves is described, numerical results are presented, and the behavior of numerical solutions of the KP and eKP equations are compared and contrasted. Recommendations for the use of eKP as a viable model for 3D interactions of internal waves are made.

2 KdV, mKdV, KP, and mKP

The derivation of KdV and KP from the governing equations for inviscid single- or two-layer flow is not trivial. Here, the equations are simply stated for a two-layer model (without rotation), and the dependence of coefficients on physical parameters is stated as well. See [9] for a derivation.

Korteweg-de Vries and Kadomtsev-Petviashvili

It makes sense to first present the KdV and KP equations for 2-layer internal waves, although it will be seen briefly that these are often not the best equations to use. Let $\hat{h}_i$ ($i = 1,2$) be the equilibrium depths of the layers. There are three relevant parameters:

$$A \equiv \frac{a}{h_0},\ B \equiv \left(\frac{h_0}{L_x}\right)^2,\ \Gamma \equiv \left(\frac{L_x}{L_y}\right)^2 \qquad \left(h_0 = \frac{\hat{h}_1\hat{h}_2}{\hat{h}_1+\hat{h}_2}\right), \tag{1}$$

where a is the scale of the wave amplitude, and L_x and L_y are the length scales in the x- and y-directions. These parameters are all assumed small. If they are of the same order, then neglecting lower order terms within the governing equations leads to the KP equation, given here in dimensional form:

$$\left(\eta_t + (c_0 + \hat{\alpha}_1\eta)\,\eta_x + \hat{\beta}\eta_{xxx}\right)_x + \hat{\gamma}\eta_{yy} = 0, \tag{2}$$

where η is the interfacial disturbance. A rigid lid and flat bottom have been assumed. The coefficients are known functions of the stratification and equilibrium layer depths:

$$\hat{\alpha}_1 = \frac{3}{2}c_0\frac{\hat{h}_1-\hat{h}_2}{\hat{h}_1\hat{h}_2},\quad \hat{\beta} = \frac{c_0\hat{h}_1\hat{h}_2}{6},\quad \hat{\gamma} = \frac{1}{2}c_0,\quad c_0^2 = g'\hat{h}_0,\quad \hat{h}_0 = \frac{h_1h_2}{h_1+h_2}, \tag{3}$$

where c_0 is the linear wave speed and g' is the reduced gravity. If we scale η, x and y by $H = \hat{h}_1 + \hat{h}_2$, t by H/c_0, and let $h_i = \hat{h}_i/H$ ($i = 1,2$), and furthermore make the change of variables $(x, t \to x - t, t)$, so that we are in a slowly evolving frame moving at the linear wave speed, (2) becomes

$$(\eta_t + \alpha_1 \eta\eta_x + \beta\eta_{xxx})_x + \gamma\eta_{yy} = 0, \tag{4}$$

$$\alpha_1 = \frac{3}{2}\frac{h_1 - h_2}{h_1 h_2}, \quad \beta = \frac{h_1 h_2}{6}, \quad \gamma = \frac{1}{2}. \tag{5}$$

It should be underlined that formally, the KP equation describes propagation of two or more waves in *nearly* the same direction (in this case, positive x). Propagation cannot be in the negative x direction. The angle with the x-axis must be small. This is the difference between *glancing* interactions of plane waves (where there is a small, but nonzero, angle between propagation directions) and *oblique* interactions (where the angle is not small). This is important to keep in mind because closed-form solutions to (4) exist and are not limited by these constraints.

If there are no transverse effects (if $L_y = \infty$, $\gamma \to 0$), then (4) reduces to the KdV equation:

$$\eta_t + \alpha_1 \eta\eta_x + \beta\eta_{xxx} = 0. \tag{6}$$

Extended KdV and Extended KP

In many situations, α_1 can be small. If it is small enough (formally, if it is $\mathrm{O}(A)$), then in order to balance dispersion with advection the regime of interest becomes $B \sim \mathrm{O}(A^2)$, and a higher order term is included:

$$\left(\eta_t + \alpha_1 \eta\eta_x + \alpha_2 \eta^2 \eta_x + \beta\eta_{xxx}\right)_x + \gamma\eta_{yy} = 0, \tag{7}$$

$$\alpha_2 = \frac{3}{(h_1 h_2)^2}\left[\frac{7}{8}(h_1 - h_2)^2 - \frac{h_1^3 + h_2^3}{h_1 + h_2}\right]. \tag{8}$$

The coefficient α_2 is negative definite. Again, neglecting transverse variation gives the eKdV equation,

$$\eta_t + \alpha_1 \eta\eta_x + \alpha_2 \eta^2 \eta_x + \beta\eta_{xxx} = 0. \tag{9}$$

3 Solitary Wave Interactions

Equation (7) has the following solitary wave solution [4]:

$$\eta = \frac{\eta_0}{b + (1-b)\cosh^2\left[k\left(x + my - ct\right)\right]}, \tag{10}$$

where the above parameters satisfy the relations

$$b = \frac{-\alpha_2 \eta_0}{2\alpha_1 + \alpha_2 \eta_0}, \; k = \sqrt{\frac{\hat{c}}{4\beta}}, \; \hat{c} = \frac{\eta_0}{6}\left(2\alpha_1 + \alpha_2 \eta_0\right), \; c = \hat{c} + \gamma m^2. \tag{11}$$

Here η_0 is the wave amplitude, k is the wavenumber in the x-direction, c is the phase speed, and m is the aspect ratio, that is, the tangent of the angle between the direction of propagation and the x-axis. Note that (10) and (11) reduce to solitary waves for the

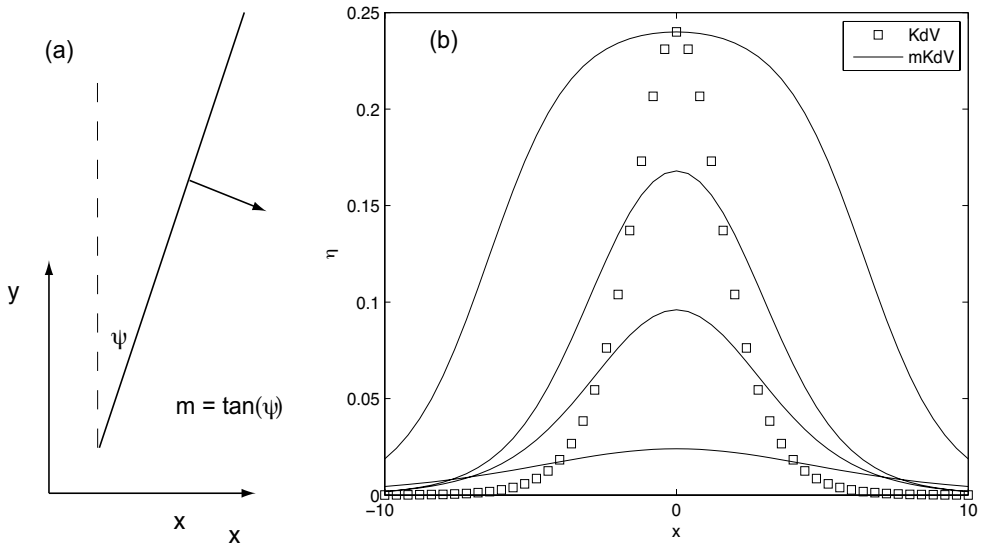

Figure 1: (a) A wave crest (solid line), or plane wave, propagating at an angle θ to the x-axis. (b) exact solitary wave solutions. A single KdV solitary wave (plus signs) is compared with eKdV solitary waves (solid lines) of different amplitudes, all less than $\eta_{0,max} = 0.2524$.

KP ($\alpha_2 = 0$), eKdV ($m = 0$), and KdV ($\alpha_2 = m = 0$) equations. Also note that, while the KP and eKP equations describe (weakly) 2-dimensional systems, the above solution is essentially 1-dimensional. For $\alpha_2 \leq 0, \eta_0\alpha_1 > 0$. That is, η_0 carries the sign of α_1, so for definiteness we assume α_1 is positive. Also, when α_2 is negative, as is generally the case for internal waves, η_0 has a maximum value of

$$\eta_{0,max} = -\alpha_1/\alpha_2. \tag{12}$$

Figure 1(a) shows the configuration of the wave. The crest moves in the positive x-direction with angle ψ to the y-axis. (m is equal to $\tan(\psi)$.) Figure 1(b) shows a KdV solitary wave (at a given y) against several eKdV solitary waves of varying amplitudes, all of which are less than the maximum amplitude given above. Putting terminology introduced earlier in context, we will talk about waves with smaller ψ (smaller m) as glancing and with larger ψ (larger m) as more oblique.

The interactions of multiple solitary waves traveling in the same direction (same m) have interesting behavior. A large-amplitude wave that is initially behind a small-amplitude wave will travel faster and eventually catch up with the smaller wave. When that happens, there is a transient nonlinear interaction, but each wave asymptotically retains its identity and structure as $t \to \infty$, except for a positive and negative phase shift of the larger and smaller wave, respectively (figure 2). KdV and eKdV solitary waves exhibit this behavior, as do KP and eKP solitary waves traveling in the same direction (but as mentioned above, the latter two cases essentially reduce to KdV and eKdV).

This solution is also interesting because it can be described by an exact analytical

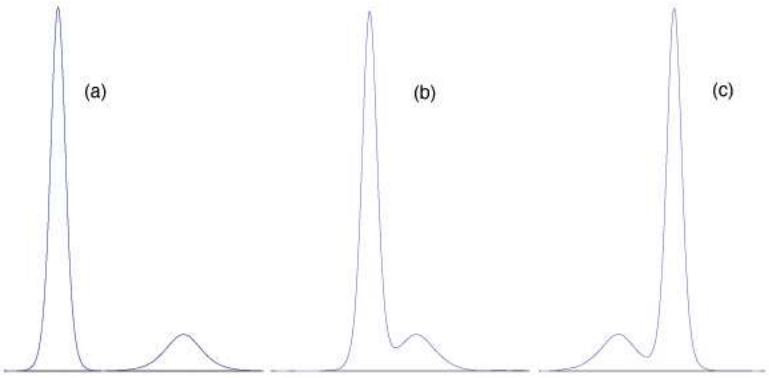

Figure 2: Interaction of two eKdV solitary waves. The larger wave, initially behind (a), eventually passes through the smaller one (b), but the two waves asymptotically retain their identity (c).

solution. In general, trains of N solitary KdV or eKdV waves (where N is finite) can be described by inverse scattering theory [11] or by Hirota's Bilinear Method ([11], or [5]). The former is more powerful, but the latter is algebraic in nature and very easy to apply. Hirota's method involves finding a dependent-variable transform of the equations such that the solitary wave solutions have the form of exponentials.

Exact solution for KP reflection

It turns out that Hirota's method also yields exact solutions of the KP equation (2) for two-dimensional solitary wave interactions. Miles ([6],[7]) derived the interaction pattern and investigated its properties, and found behavior qualitatively different than the 1-D case. We first summarize Miles's solution. Given two solitary wave solutions to the KP equations with wavenumbers k_i $(i = 1, 2)$, and propagation directions such that their angles with respect to the x-axis have tangents m_i, the following solution is found [8]:

$$\eta = \left(\frac{48\beta}{\alpha_1}\right) \frac{k_1^2 e^{-2\theta_1} + k_2^2 e^{-2\theta_2} + (k_1 - k_2)^2 e^{-2\theta_1 - 2\theta_2} + A_{12}\{(k_1 + k_2)^2 + k_2^2 e^{-2\theta_1} + k_1^2 e^{-2\theta_2}\} e^{-2\theta_1 - 2\theta_2}}{\left[1 + e^{-2\theta_1} + e^{-2\theta_2} + A_{12} e^{-2\theta_1 - 2\theta_2}\right]^2}, \tag{13}$$

where

$$\theta_i = k_i \left(x + m_i y - c_i t\right), \quad A_{12} = \frac{(m_1 - m_2)^2 - \frac{12\beta}{\gamma}(k_1 - k_2)^2}{(m_1 - m_2)^2 - \frac{12\beta}{\gamma}(k_1 + k_2)^2}, \tag{14}$$

and c_i, k_i, m_i satisfy (11) with $\alpha_2 = 0$. There are several things to notice about this solution. First, since the phase lines are not aligned, we can take the limit $\theta_2 \to 0$ or ∞ with θ_1 constant (and vice versa), and this limit has the form (10); that is, the waves retain their identities after interacting with each other. Second, the interaction parameter A_{12} can be negative when

$$(m_1 - m_2) \in \left(\sqrt{\frac{12\beta}{\gamma}}(k_1 - k_2), \sqrt{\frac{12\beta}{\gamma}}(k_1 + k_2) \right) \equiv (2m_-,\ 2m_+)\,, \tag{15}$$

and it turns out that solutions in this parameter range, while mathematically admissable, are nonphysical (this point will be returned to briefly). Third, the interaction can be much larger in amplitude than a superposition of the two waves. In fact, for waves of the same amplitude, the amplitude increase can be up to four-fold, as compared with a two-fold increase from linear superposition.

Slightly changing focus, we can consider the kinematic resonance condition for three solitary waves:

$$k_1 \pm k_2 = k_3,\ m_1 k_1 \pm m_2 k_2 = m_3 k_3,\ \omega_1 \pm \omega_2 = \omega_3 \quad (\omega_i = c_i k_i), \tag{16}$$

where ω is frequency. In fact, given two KP solitary waves, a third satisfying (16) exists only if one of the bounds of (15) is acheived.

It must be stressed that (16) is an algebraic constraint, and alone is not a sufficient condition for resonant interaction of solitary waves. However, Miles showed that the limiting form of (13), as the upper bound of (15) is approached, is equal to

$$\eta = \left(\frac{48\beta}{\alpha_1} \right) \frac{k_1^2 e^{2\theta_1} + k_2^2 e^{-2\theta_2} + (k_1 + k_2)^2 e^{2\theta_1 - 2\theta_2}}{\left[1 + e^{2\theta_1} + e^{-2\theta_2}\right]^2}. \tag{17}$$

Furthermore, it can be shown that this solution is asymptotic to three interacting waves – the two waves considered in (13) and a third wave that is resonant with the first two. This can be shown by holding constant one of each of the three phase variables involved, and letting the other two go to zero or ∞. Figure 3 shows (13) both for an oblique interaction and for a near-resonant interaction. Both are symmetric, i.e. $k_1 = k_2$ and $m_1 = -m_2$. The large interaction in 3(b) resembles a third resonant wave, although it is not actually a resonant wave until the angle predicted by (15) is reached.

The above discussion can be applied to glancing reflections of solitary waves against a wall. The results are the same since the condition of no normal flow ($\eta_y = 0$) at the wall allows one to extend the solutions by symmetry. The theory allows for regular reflection, as described by (13) with $k_1 = k_2$ and $m_1 = -m_2$, for $m_1 > m_{res}$, where

$$m_{res} \equiv \sqrt{\frac{12\beta}{\gamma}} k_1 = \sqrt{\frac{\alpha_1 \eta_0}{\gamma}}, \tag{18}$$

where η_0 is the amplitude of the incident wave. If, however, $m_1 \leq m_{res}$, regular reflection is no longer allowed. Instead, the interaction is described by (17), where the subscripts 1 and 2 correspond to the incident and reflected waves, respectively, and a third wave is resonant. This third wave, which has no transverse wavenumber and travels parallel to the wall, is know as the **mach stem** by analogy with a phenomenon seen in gas dynamics. Since the transverse wavenumber of the mach stem is zero, and the waves are in resonance, the amplitude of the mach stem and of the reflected wave can be inferred from the kinematic resonance constraint (16):

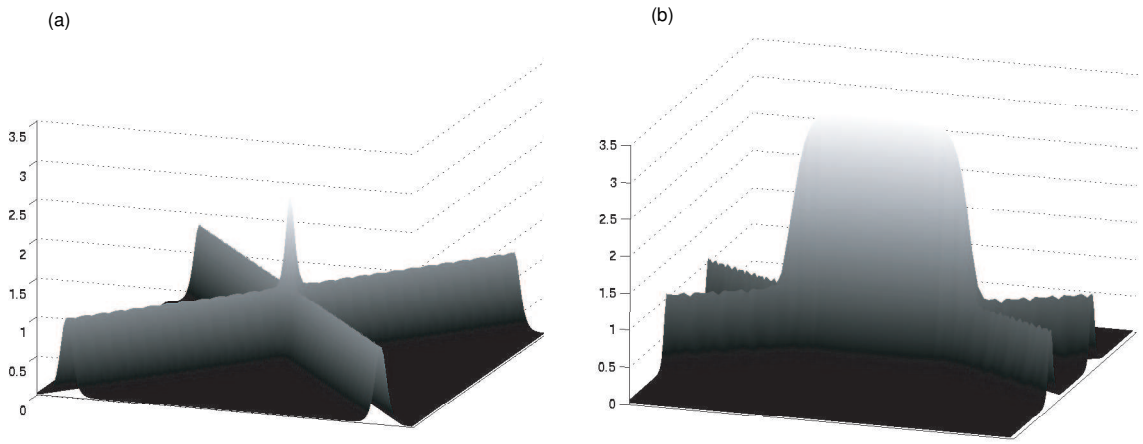

Figure 3: (a) Oblique interaction. (b) Near-resonant interaction.

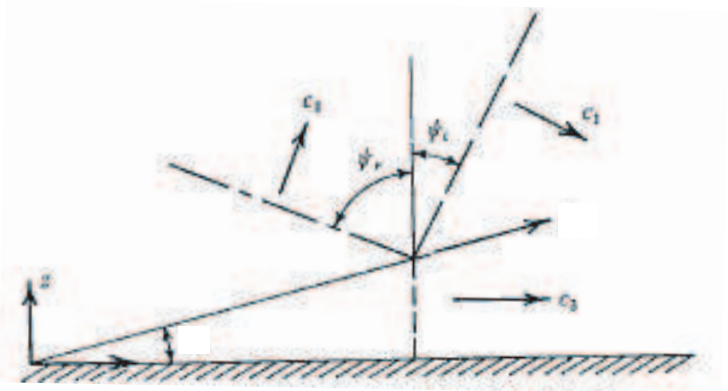

Figure 4: Mach reflection. The incident wave (– –) moves into the wall with phase velocity c_1, and the reflected wave (– - –) moves away at c_2. The intersection of the incident and reflected waves with the mach stem (—) moves away from the wall. Taken from [7].

$$m_2 = m_{res},\ k_2 = k_1\frac{m_1}{m_{res}},\ \eta_{0,2} = \frac{12\beta}{\alpha_1}k_2^2,\ k_{mach} = (1+\frac{m_1}{m_{res}})k_1,\ \eta_{0,mach} = \frac{12\beta}{\alpha_1}k_{mach}^2. \quad (19)$$

In this case, if $k_2 < k_1$, the interaction pattern will move away from the wall with time, and thus the mach stem will grow in length. This configuration is shown in figure 4. The maximum amplitude, or *runup*, at the wall can then be calculated as a function of m:

$$\frac{\eta_{max}}{\eta_0} = \begin{cases} 4\left(1+\sqrt{1-(m_{res}/m)^2}\right)^{-1} & m > m_{res} \\ (1+m/m_{res})^2 & m < m_{res} \end{cases}, \quad (20)$$

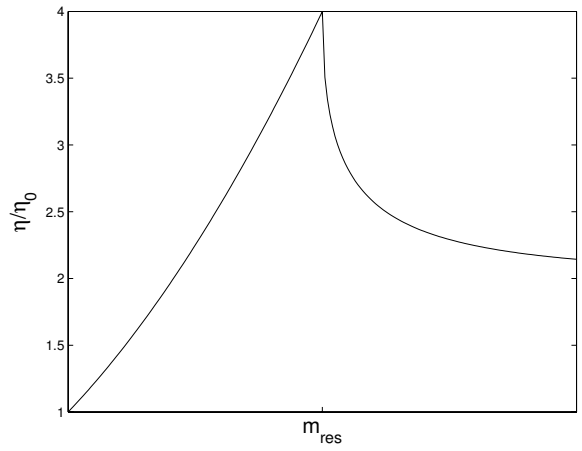

Figure 5: Theoretical KP runup at wall versus m (tangent of incident angle)

(see figure 5), which is useful since it is easy to verify by lab or numerical experiment.

Modified KP Interactions

It may be apparent to the reader that the word *soliton* has not used liberally up to this point, although the term applies to the interacting solitary waves described above. One can use the term to describe solitary waves that can pass through each other and still retain their identity, in which case the term applies, in a very limited way, to eKP solitary waves (see below). But one could also think of solitons in a loose sense as solitary wave solutions that are amenable to the various transform methods (e.g. Hirota's Bilinear method) used to make analytical headway in describing their interactions. It is shown in [2] that the same bilinear transform methods that work quite well on KdV, eKdV, and KP (as well as many other nonlinear wave equations that support solitons) break down when applied to the eKP equation, except for the degenerate case in which all solitary waves are traveling in the same direction. Further, it can be shown that the eKP equation does not pass the Painlevé test, a criterion in determining whether an equation is completely integrable. This does not prove that eKP is non-integrable, but it demonstrates that exact solutions will, at the very least, not be easy to find. For that reason, the focus of this study is numerical in nature; since (20) predicts a large amplitude increase, while (10) gives a maximum amplitude constraint when a cubic term is present, it is unclear what the results of such an experiment will be.

4 Numerical Model

There is a difficulty inherent in solving (7) numerically. If we integrate the equation in x, assuming that disturbances are locally confined, then

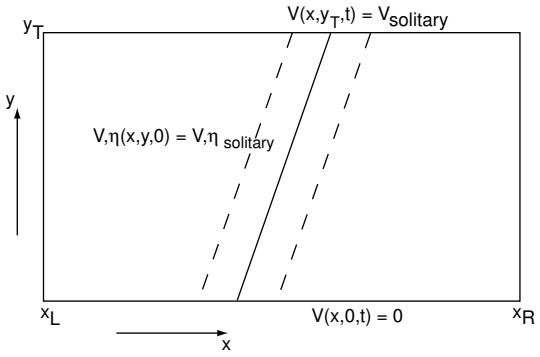

Figure 6: Model schematic.

$$\int_{-\infty}^{\infty} \eta_{yy}(x,y,t)dx = \frac{\partial^2}{\partial y^2}\int_{-\infty}^{\infty} \eta dx = 0, \tag{21}$$

a condition known as the "mass condition." In particular, a given initial condition must satisfy this constraint; otherwise it can be shown there are waves present with infinite group speed which propagate to $x = -\infty$ [1]. Alternatively, one can examine the evolution equation that results from an integration in x:

$$\eta_t + \alpha_1\eta\eta_x + \alpha_2\eta^2\eta_x + \beta\eta_{xxx} - \gamma\int_x^{\infty} \eta_{yy}dx = 0. \tag{22}$$

If a discretized form of (21) is not satisfied, then disturbances will appear instantaneously far behind the initial condition. To avoid this problem, eKP is written in the form given in section 2, but with the time derivative left in the y-momentum equation [9]:

$$\eta_t + \alpha_1\eta\eta_x + \alpha_2\eta^2\eta_x + \beta\eta_{xxx} + \gamma V_y = 0, \tag{23}$$

$$V_t - V_x + \eta_y = 0. \tag{24}$$

The time derivative is neglected in the derivation of eKP for asymptotic consistency, but here is left in in order to regularize the equation, and the numerical model now solves for both η and V.

Most of the numerical experiments involved a single solitary wave with a transverse component ($m \neq 0$) directed into a wall ($y = 0$) as an initial condition. In this case V was held at zero at $y = 0$ for all t, and was set to the analytical solution for such a wave at y_T, which was effectively considered to be $y = +\infty$ (figure 6). η and V were solved on grids that were coincident in x but staggered in y. In the y-direction, the topmost and bottom-most points were V-points, so boundary conditions were imposed on V but not on η (unless the domain was doubly-periodic). Spatial derivatives were approximated by centered differences. First derivatives in x were 4th order, while all others were 2nd order. The nonlinear terms were approximated by straightforward multiplication (no averaging was done). The timestepping scheme was an Adams-Bashforth predictor-corrector method involving two previous timesteps, where the two initial steps were done by Heun's method.

Very often a simulation was restarted using the final state as a new initial condition; in this case the two previous timesteps were not saved. A few doubly-periodic simulations were done where the initial condition was a superposition of different solitary waves, but the bulk of the numerical experiments done were with the wall model described above.

Since no wave was expected to propagate faster than the incident wave, η and V were set to zero at x_R. However, conditions at x_L were not as straightforward, and were handled as follows: the solution on the first two gridpoints in the x-direction was extrapolated linearly backward. This was in order to allow any disturbances, which presumably would be traveling to $x = -\infty$ in the frame in which (23) and (24) are defined, to pass through x_L rather than reflect back into the domain. In addition, a linear damping of the form

$$\begin{aligned} \eta_t &= \ ... \ - \mu(x)\eta \\ V_t &= \ ... \ - \mu(x)V \end{aligned}$$

was added, where μ (≥ 0) is nonzero only in a small neighborhood of x_L. This is justified physically by the assumption that the incident wave, its reflection, and their interaction are the fastest-moving disturbances in the system, and so long as they are sufficiently resolved away from x_L, then what happens near x_L should not affect their behavior. Resolution was often higher in x than in y. The timestep was made short enough to avoid a CLF-type instability. The upper bound was determined more empirically than by theoretical means due to the nonlinearity of the equations.

A simple rescaling (not given here) of η, x, y and t (where x and y are scaled identically so that angles are preserved) allows us to replace α_1, β, and γ as given in section 2 with any values we choose. For programmatic ease, these parameters were set to 1.5, 0.125, and 0.5, respectively. Values of α_2 were found by (8) and then applying the same scaling.

5 Numerical Results

In the wall experiment, if η is scaled to the amplitude of the incident wave, η_0, then (23) becomes

$$\hat{\eta}_t + \alpha_1 \eta_0 \left(\hat{\eta} - \frac{\eta_0}{\eta_{0,max}} \hat{\eta}^2 \right) \hat{\eta}_x + \beta \hat{\eta}_{xxx} \ ... \tag{25}$$

where $\eta_{0,max}$ was defined in section 3. If the nondimensional parameter $\eta_0/\eta_{0,max}$ is zero, we recover KP (or, according to our model, a regularized version of KP), so the larger this parameter, the more departure we expect from KP reflection behavior. So numerical experimentation began by benchmarking the numerical model's ability to reproduce known results. Except where explicitly stated, the values of α_1, β and γ in all of the experiments described below were 1.5, 0.125, and 0.5, respectively, and α_2 was computed using $h1 = 0.67$.

Unidirectional eKP

As mentioned above, one should be able to generate a 2-soliton solution to the eKP equation, as long as both solitary waves are traveling in the same direction. Though it does not involve reflection, this is still an important result. A doubly periodic domain was used, with a large

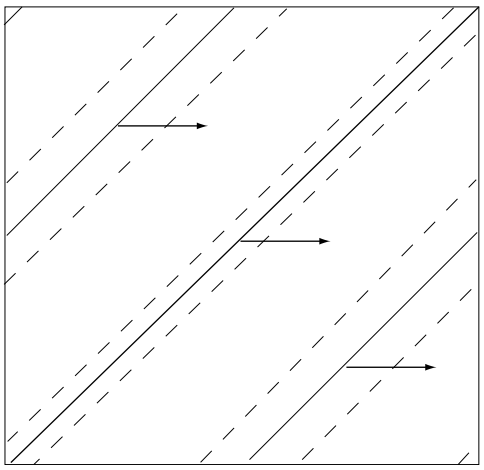

Figure 7: Doubly periodic domain used to simulate eKP soliton interactions. The initial condition is shown here; the narrower wave crest is larger in amplitude.

wave behind a small wave as an initial condition (figure 7). This simulation was shown to produce the typical 1-D soliton interaction pattern. Figure 2 actually shows cross-sections of snapshots of this simulation for $m = 0.4$.

KP and eKP Reflection

Figures 8(a)-8(c) show the development of a KP interaction pattern for different incident angles. In all KP experiments, the incident amplitude $\eta_0 = 0.12$, $m_{res} = 0.6$. Figures are shown for $m_{incident}$ greater than, equal to, and less than the resonant value. For $m_{incident} = 0.8$, the reflection pattern is symmetric, with the maximum wall amplitude $\approx 2.6\eta_0$. For $m_{incident} = 0.6$, the resonant angle, we see a mach stem slowly forming with amplitude close to $4\eta_0$. Theory predicts a mach stem will not grow at the resonant angle, and that the maximum amplitude achieved is $4\eta_0$; however, since this is a numeric approximation it is perhaps not surprising that resonance is not acheived exactly. The fact that stem growth is very slow and amplitude increase is close to 4 is encouraging. At $m_{incident} = 0.15$, the reflected wave is difficult to see because it is so small and obscured by its own reflection from the far wall. It is, as predicted, clearly at a far more oblique angle than the incident wave. Also, the mach stem has an amplitude $\eta_{wall} = 1.6\eta_0$ that is very close to that of the incident wave.

It should be stressed that the theory concerns stationary solutions, not transient development from arbitrary initial conditions. Comparing transient solutions for $m_{incident} = 0.6$ with those for $m_{incident} = 0.8$ and $m_{incident} = 0.15$ shows that a near-resonant interaction takes a long time to develop. This can be seen by plotting the maximum wall amplitude of η at the wall as a function of time. This is shown for the same simulations in figure 8(d). All of the plots show convergence to a stationary amplitude. The small oscillations around this mean can be explained by failure to completely resolve the peak of the wave crest; however, this is likely not detrimental to the overall solution.

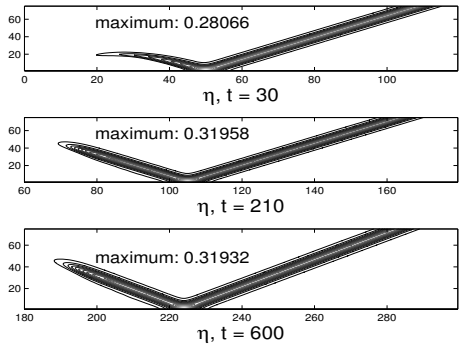

(a) $m_{incident} = 0.8$. Reflection is regular.

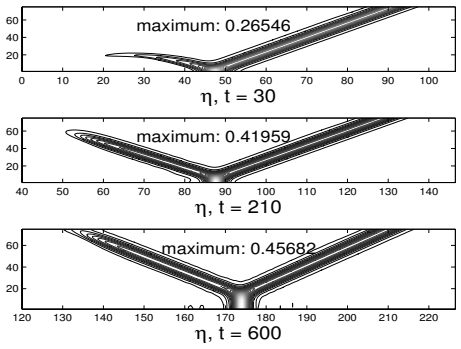

(b) $m_{incident} = 0.6$. Reflection is near-resonant. Note maximum amplitude and beginning of mach stem formation.

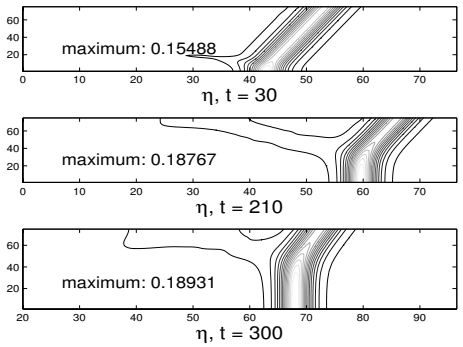

(c) $m_{incident} = 0.15$. Mach Reflection. Note fully-developed mach stem which grows in time.

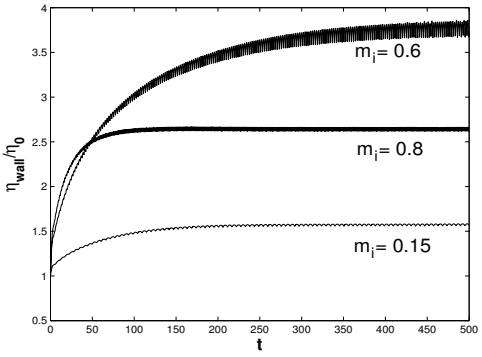

(d) Maximum amplitude versus time for all three simulations. Oscillations likely from failure to fully resolve highest peak.

Figure 8: KP reflection, $\eta_0 = 0.12$.

Figures 9(a)-9(c) show analogous results for eKP interactions with $\eta_0 = 0.12$. A value of 0.67 was chosen for h_1 as given in section 2, giving $\eta_{0,max} = 0.2524$, and $\eta_0/\eta_{0,max} \approx 0.48$. Comparing figures 8(a) and 9(a), we again see regular reflection, but the interaction amplitude is smaller for the eKP case, and in fact is smaller than $\eta_{0,max}$. Figure 9(b), resulting from an incident angle with tangent 0.45, appears to show a reflected wave with angle equal to the incident, trailed by smaller crests with more oblique angles, in contrast with the mach reflection pattern that would be seen with KP, and a maximum amplitude just greater than $\eta_{0,max}$. For $m_{incident} = 0.15$, shown in figure 9(c), we do see a pattern that looks qualitatively like mach reflection, although it is not clear whether this term actually applies to the interaction. Still, with relatively little apparent transverse variation near the wall, one can anticipate that the profile at the wall looks very similar to an eKdV solitary

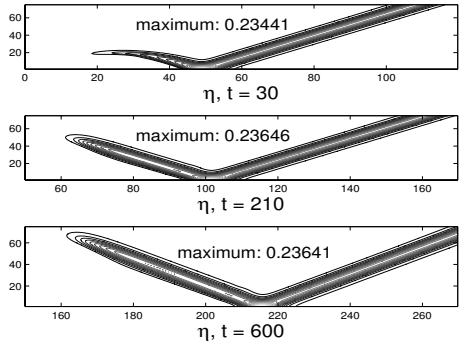

(a) $m_{incident} = 0.8$. Reflection is regular.

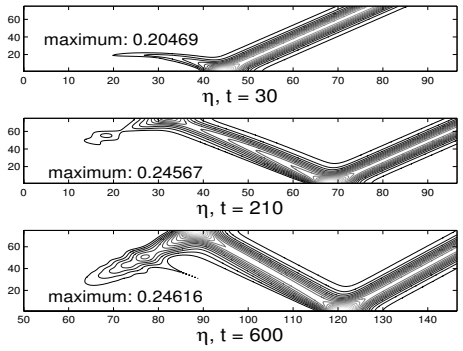

(b) $m_{incident} = 0.45$. Maximum amplitude is near $\eta_{0,max}$ (see figure 10(c)). Note smaller, more oblique wave crests trailing the reflected wave.

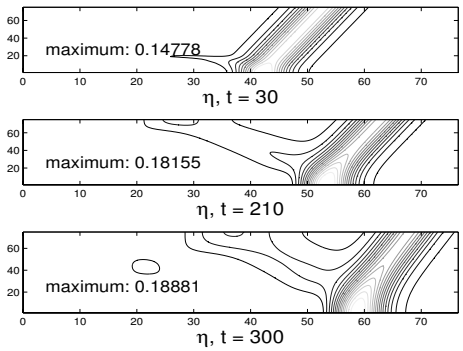

(c) $m_{incident} = 0.15$. Interaction pattern resembles mach reflection.

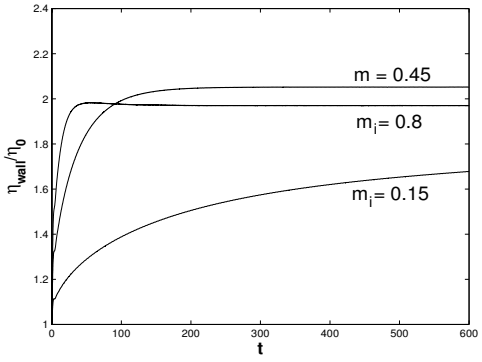

(d) Maximum amplitude versus time for all three simulations.

Figure 9: KP reflection, $\eta_0 = 0.12$, $h_1 = 0.67$ (see section 2).

wave, and this was found to be the case.

Comparing the maximum runup of KP simulations to theory, figure 10(a), we see very good agreement for angles less than the resonant angle. However, for angles larger than the resonant angle the agreement is not so good. This is certainly an issue, and may be a consequence of the use of regularized equations (see Discussion section). Still, all of the qualitative aspects of the theory were captured, and for small angles the quantitative agreement was good as well.

Figure 10(b) shows the same results as figure 10(a) along with the results from eKP simulations for different values of η_0, where $m_{incident}$ has been scaled to m_{res}, as given by (18). Values of η_0 used were 0.024, 0.05, 0.12, and 0.24, while $\eta_{0,max} = 0.2524$ for all cases. Recalling (25), notice that, for $\eta_0 = 0.024$ and $\eta_0 = 0.05$ (dots and triangles, respectively),

the runup plot has a qualitatively similar shape to that of KP, but the maximum occurs at a smaller (scaled) incident angle and is not as large. The same could be said of $\eta_0 = 0.12$, though the maximum is barely visible, and we have seen qualitatively different results for this amplitude. In fact, it does seem as though the eKP runup plots may coincide with that of KP where the incident angles are small enough that $\eta_{wall} < \eta_{0,max}$. These points correspond to interaction patterns that look similar to mach reflection (cf. figure 9(c)), though there is not space to show all of the results. Again, it is stressed that the development of these interaction patterns is transient. In a few cases, the growing "mach stem" reached the far wall before the wall amplitude became stationary, and in these cases, the result given in figures 10(b), 10(c) is that taken just before this intersection occurred.

Obviously, the above statements do not apply to the case $\eta_0 = 0.24$, since $\eta_0/\eta_{0,max} \simeq 1$. Indeed, the runup plot for $\eta_0 = 0.24$ is very different than the others. Figure 10(c) shows the same results as those in figure 10(b) without scaling amplitude by η_0. Here it is seen that when $\eta_0 = 0.024, 0.05, 0.12$, the runup is never greater than $\eta_{0,max}$ (solid line), but is for $\eta_0 = 0.24$. This contrast suggests that the range $0.12 < \eta_0 < \eta_{0,max}$ should be investigated for transition between the two behaviors, but this was not done in the current study. Figure 10(d) shows the result of one of the simulations where $\eta_0 = 0.24$.

One might ask if a resonant interaction actually does occur in the eKP simulations. Though (16) is not sufficient for resonance, it is necessary and can be checked. It is easiest to check the first two conditions of (16) since they relate only to the wavenumbers and not the phase speeds, and wavenumbers are calculated from amplitudes using (11). Further, the requirement that one of the bounds of (15) be satisfied for the kinematic resonance condition to apply holds for eKP as well as KP. This can be observed as follows. Consider two (1 and 2) solitary wave solutions to eKP. Imagine that both wavenumbers (k_1 and k_2) are known, and the direction of the first (m_1) is known (but not of the second), and the waves are constrained to satisfy (16) for some solitary wave with wavenumber and direction k_3 and m_3. From (11), we can give wavenumbers in terms of frequencies and propagation directions:

$$4\beta k_i^2 = \frac{\omega_i}{k_i} - \gamma m_i^2, i = 1, 2. \tag{26}$$

Together with (16), these two equations form a set of 5 algebraic equations for the unknowns $m_2, m_3, k_3, \omega_2, \omega_3$, which can then be solved for two possible values of m_2. The important thing to notice is that the above equations do not depend on α_2, and so, even when eKP solitary waves are considered, the results still correspond to the bounds of (15), even though the corresponding phase velocities and amplitudes are different than the KP case.

Table 1 shows calculated wavenumbers for the incident and reflected waves, as well as the mach stem, assuming solitary wave solution (10). (The term "mach" is used here for lack of a better one; as mentioned before, the eKP simulations show behavior qualitatively like mach reflection.) As in Miles' analysis, for KP we assume that the mach stem is at right angles to the wall and the the reflected angle is the resonant angle, i.e. $m_{mach} = 0$ and $m_{refl} = m_{res}$. By inspection, we also set $m_{mach} = 0$ for eKP, but with out an exact solution there is no reason to assume $m_{refl} = m_{res}$, and so m_{refl} had to be measured. This measurement is done by examination of the numerical solution of η. However, the reflected wave crest is often either not fully developed, obscured by the far wall or the stem crest,

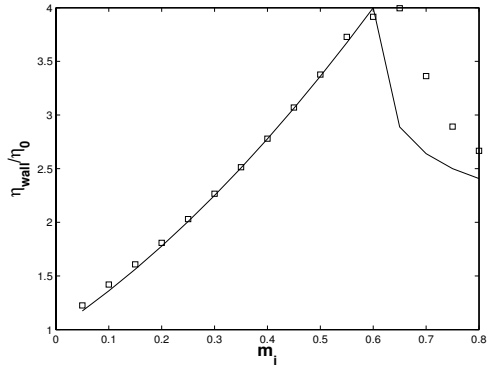

(a) KP reflection runup. Comparison of results with theory.

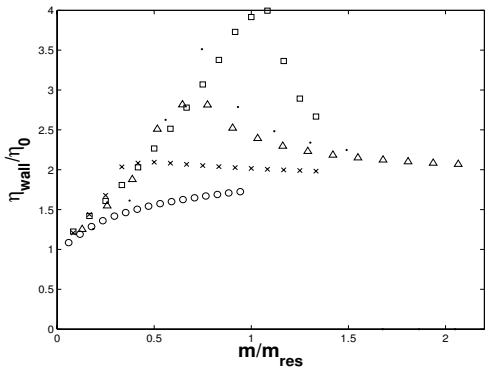

(b) eKP reflection runup for different values of η_0: 0.24 (circles), 0.12 (x's), 0.05 (triangles), 0.024 (dots), compared with KP runup, $\eta_0 = 0.12$ (squares). Values are normalized by η_0.

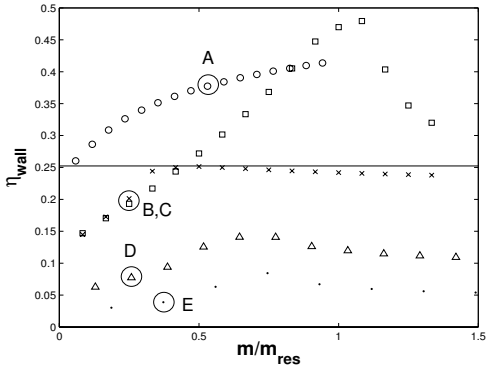

(c) Same as (b), but not normalized by η_0. Solid line is $\eta_{0,max}$. **B,C,D,E** correspond to the results in Table 1.

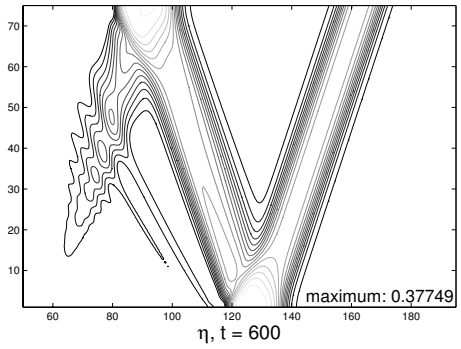

(d) eKP, $\eta_0 = 0.24$, $m_{incident} = 0.45$ (corresponds to **A** in (c). For this simulation, the wall amplitude is stationary.

Figure 10: Reflection runup

very short in length, or very small in magnitude, or all of the above. Measurement of k_{refl} is problematic for these reasons, and measurement of m_{refl} even more so. Still, there is no other method of verifying whether (16) is satisfied. It can be seen from Table 1 that agreement is not bad for KP. It is worse for eKP, but improves with decreasing amplitude.

Positive α_2

In certain cases, vertical shear and stratification can conspire to make α_2 positive [3]. Equation (10) still applies, only now the amplitude can take on either sign (we are still

Expt		k_{inc}	k_{refl}	k_{mach}	m_{refl}	$\frac{k_{inc}m_{inc}}{m_{refl}}$	$k_{inc}+k_{refl}$
KP	$\eta_0 = 0.12, m_{inc} = 0.15$	.3464	.099	.4322	0.6	.0866	.4454
eKP	$\eta_0 = 0.12, m_{inc} = 0.15$	.3011	.1385	.3412	0.52	.0869	.4396
eKP	$\eta_0 = 0.05, m_{inc} = 0.1$	.2199	.0653	.242	0.45	.0489	.2852
eKP	$\eta_0 = 0.024, m_{inc} = 0.1$	.1511	.0465	.1709	1.0	.0151	.1976

Table 1: Incident, reflected, and mach stem wavenumbers (k_{inc}, k_{refl}, and k_{mach}, resp). (the term 'mach' is used even if it is not clear that there is resonance.) Equality of the last column with k_{mach} and of the second-last column with k_{refl} is required by the kinematic resonance condition. The former criterion involves angle measurements, which are more problematic than wavenumber measurements, while the latter does not.

using the convention that α_1 is positive). If η_0 is positive, there is no maximum amplitude; if η_0 is negative, it must be larger (in absolute value) than $2\alpha_1/\alpha_2$. Several simulations were carried out with positive α_2, however the sweep of the parameter space was not nearly as complete as for negative α_2. Some results are shown in figures 11(a)-11(c). Figure 11(a) is the result of a simulation in which $\eta_0 = 0.12$ and $m_{incident} = 0.6$, as for figure 8(b). α_2 is positive and set to $+1$, and the coefficients α_1, β, and γ remain as above. We see a pattern very similar to the KP result, but with a small radiative pattern shed from both the incident and reflected waves in the bottom left corner. More interesting are the results where η_0 is negative, as in figure 11(b). Here $\eta_0 = -0.3$, and $m_{incident} = 0.4$. There is a similar radiation pattern, but it is more developed. In fact, when the profile at the wall is examined, the radiation pattern is shown to have the same profile as the incident wave, and to have traveled the same distance. F'igure 11(c) shows the development of the profile at the wall. The larger peak is the stem seen in 11(b); the smaller peak is the intersection of the radiated wave crests. When compared with figure 2, the wall profile of η looks very similar to the interaction of two unidirectional solitons. Given that transverse variation appears small near the wall in 11(b), it is perhaps not surprising that the profile at the wall is similar to an eKdV solution; however, it is surprising that interaction of the incident wave with its reflection develops into something similar to a two-soliton solution.

A result similar to figure 11(b) is shown in [10], though in that study the Modified KP equation (which is similar to eKP with positive α_2 and no quadratic term) was being investigated. Also, the profile of the intersection of the radiated wave crests was not examined in that study.

The investigation of positive α_2 was not taken further – it was meant only as a brief exploration of different behavior and possible starting point for further study.

6 Discussion

We have seen that a numerical model which gives reasonable agreement with theory concerning the glancing interaction of two KdV solitary waves (figs. 5, 10(a)) produces somewhat different behavior when two eKdV solitary waves interact, with the degree of difference depending on the magnitude of the incident amplitude relative to $\eta_{0,max}$. When the interaction amplitude is close to the maximum possible amplitude of an eKdV solitary wave, we see

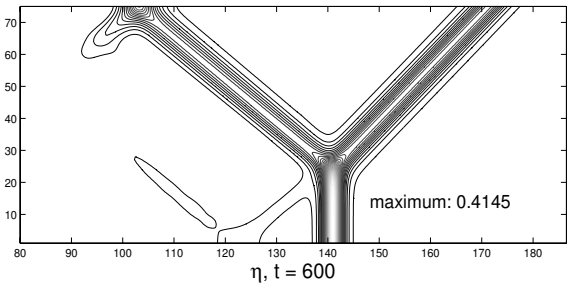

(a) eKP: $\alpha_2 = +1$, $\eta_0 = 0.12$, $m_{incident} = 0.6$. Note radiation trailing the interaction.

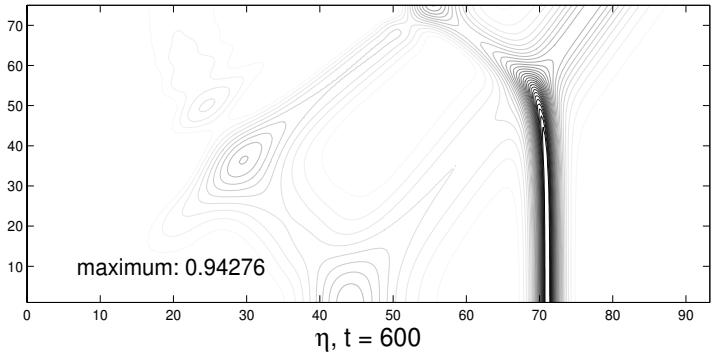

(b) eKP: $\alpha_2 = +1$, $\eta_0 = -0.3$, $m_{incident} = 0.4$. Trailing radiation more developed than in (a).

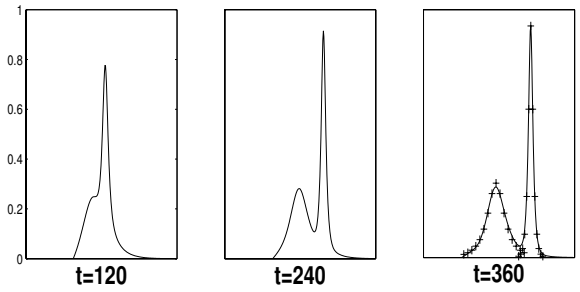

(c) Snapshots of profile at wall from simulation leading to (b). At $t = 360$, analytical solutions (+) are superimposed on profile, centered on the peaks: on the smaller peak, the boundary condition at the far wall, and on the large peak, and eKdV solitary wave with the same amplitude.

Figure 11: Positive α_2

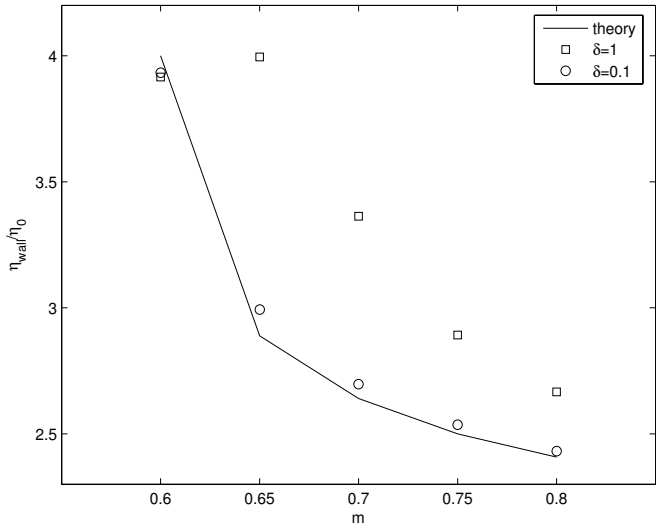

Figure 12: Runup results comparing different regularization schemes, where δ is as in (27). $\delta = 1$ corresponds to the results shown in figure 10(a), and $\delta = 0.1$ gives results closer to theory.

what appears to be dispersion occurring near the intersection of the interacting waves. This is not surprising because the nonlinear term in the eKP equation is small when amplitude is close to $\eta_{0,max}$, but there is no reason to expect the dispersive term to be small.

In some cases, the eKP simulation results in a pattern that resembles a mach stem and a nonsymmetric reflected wave, as in the KP simulations. However, it is not clear whether this is a stationary solution, or whether it is a resonance of three solitary waves. Long-time simulations (e.g. figure 9(c)) seem to suggest that such a pattern is stationary and would last until effects of the far wall became important. Table 1 suggests that the kinematic resonance condition is not satisfied. However, there are difficulties in measuring the properties leading to this conclusion. We have also seen that when the incident amplitude is near the maximum amplitude (figs. 10(d), 10(c)) the interaction does not resemble KP interaction at all.

It was suggested above that the disagreement with theory with respect to wall amplitude in KP reflection when $m_{incident} > m_{res}$ (figure 10(a)) may be a result of regularization in the numerical model. This claim was investigated by generalizing (24) to

$$\delta V_t - V_x + \eta_y = 0, \tag{27}$$

where δ is a parameter between 0 and 1. Preliminary results (figure 12) show better agreement with theory for $m_{incident} > m_{res}$ when δ is small.

7 Conclusions and further work

One of the early goals of this study was to find a closed form solution for the eKP equation (aside from the degenerate one where all waves move in the same direction). The literature

seemed to suggest that such a solution would be extremely difficult to find. Indeed, the fact that some results were highly dispersive seems to indicate that the eKP equation, unlike the KP equation, does not have soliton solutions for three dimensional solitary wave interactions.

That issue aside, the results of this study constitute a tool to gauge the KP and eKP equations as representative models of internal waves with small transverse variation. Oceanographic data was not used in this study; however, the two models exhibit qualitatively different behavior, and this behavior can be compared with that of actual internal solitary waves. For instance, tidal flow over bathymetry may cause glancing internal solitary wave interaction with some regularity, and might be useful to be able to predict the nonlinear amplitude increase based on known parameters such as stratification and background currents.

The results shown in figure 12 suggest that the disagreement with theory shown in figure 10(a) is due to regularization, and that a different regularization such as (27) with δ small might yield better agreement. However, this must be investigated further, and this investigation is the subject of ongoing work.

The investigation of the eKP equation with positive α_2 was not very extensive, but it still yielded interesting results. There were small radiative waves in all eKP simulations (including those with negative α_2, although they are not visible in the plots shown), but we saw from figures 11(b), 11(c) that these radiative waves may have interesting structure. Further analysis of the parameter space is certainly warranted.

References

[1] Akylas, TR, 1994. Three-dimensional long water-wave phenomena. *Annu. Rev. Fluid Mech.* **26**, 191-210.

[2] Chen Y, P Liu, 1998. A generalized modified Kadomtsev-Petviashvili equation for interfacial wave propagation near the critical depth level. *Wave Motion* **27** (4), 321-339.

[3] Grimshaw R, E Pelinovsky, T Talipova, A Kurkin, 2004. Simulation of the transformation of internal solitary waves on oceanic shelves. *J. Phys. Oceanogr.* **34**, 277491.

[4] Helfrich, K and K Melville, 2006. Long nonlinear internal wave. *Annu. Rev. Fluid Mech.* **38**, 395-425.

[5] Hirota, R. The Direct Method in Soliton Theory. Cambridge University Press, 2004.

[6] Miles, J, 1977. Obliquely interacting solitary waves. *J. Fluid Mech.* **79**, 157-169.

[7] Miles, J, 1977. Resonantly interacting solitary waves. *J. Fluid Mech.* **79**, 171-179.

[8] Soomere, T and J Engelbrecht, 2006. Weakly two-dimensional interaction of solitons in shallow water. *European Journal of Mechanics B*, in press.

[9] Tomasson, GG, 1991. Nonlinear waves in a channel: Three-dimensional and rotational effects. Doctoral Thesis, M.I.T.

[10] Tsuji, H and M Oikawa, 2004. Two-dimensional Interaction of Solitary Waves in a Modified KadomtsevPetviashvili Equation. *J. Phys. Soc. Japan.* **73** (11), 3034-3043.

[11] Whitham, GB. Linear and Nonlinear Waves. John Wiley and Sons, 1974.